

# Reactivity Patterns of O<sub>2</sub>, CO<sub>2</sub>, Carboxylic Acids, and Triflic Acid with Molybdenum Silyl Hydrido Complexes Bearing Polydentate Phosphinoalkyl–Silyl Ligands: Pronounced Effects of Silyl Ligands on Reactions

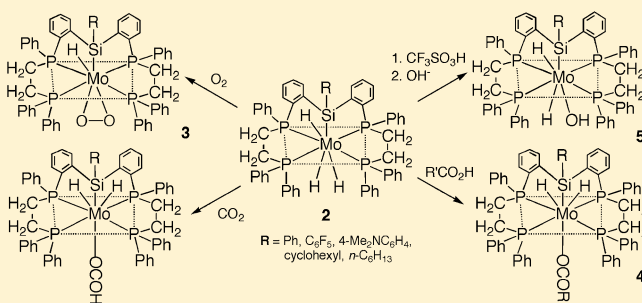
Makoto Minato,<sup>\*,†</sup> Da-Yang Zhou,<sup>†,§</sup> Ken-ichiro Sumiura,<sup>†</sup> Yuki Oshima,<sup>†</sup> Shigeki Mine,<sup>†</sup> Takashi Ito,<sup>†</sup> Masaki Kakeya,<sup>†</sup> Kei Hoshino,<sup>†</sup> Takahiro Asaeda,<sup>†</sup> Takushi Nakada,<sup>†</sup> and Kohtaro Osakada<sup>‡</sup>

<sup>†</sup>Department of Materials Chemistry, Graduate School of Engineering, Yokohama National University, 79-5 Tokiwadai, Hodogaya-ku, Yokohama, 240-8501, Japan

<sup>‡</sup>Research Laboratory of Resources Utilization, Tokyo Institute of Technology, 4259, Nagatsuta, Midori-ku, Yokohama, 226-8503, Japan

## S Supporting Information

**ABSTRACT:** The reactivity patterns of a series of molybdenum silyl hydrido complexes, [MoH<sub>3</sub>{[Ph<sub>2</sub>PCH<sub>2</sub>CH<sub>2</sub>P(Ph)-C<sub>6</sub>H<sub>4</sub>-o]<sub>2</sub>(R)Si-P,P,P,P,Si}] (2a, R = Ph; 2b, R = C<sub>6</sub>F<sub>5</sub>; 2c, R = 4-Me<sub>2</sub>NC<sub>6</sub>H<sub>4</sub>; 2d, R = cyclohexyl; 2e, R = *n*-C<sub>6</sub>H<sub>13</sub>), toward electrophilic materials, including dioxygen, carbon dioxide, carboxylic acids, and triflic acid, have been explored. The influence of substituents directly attached to the Si atom in the quintuply chelating diphosphine–silyl ligands during the course of the reactions has been studied in detail. Complexes 2a–c react readily with dioxygen at ambient temperature, yielding η<sup>2</sup>-O<sub>2</sub> complexes 3a–c, in which the dioxygen ligand ligates at the site opposite to the Si atom. Single-crystal X-ray studies have established that the Mo–O distance of 3a, which contains a phenyl-substituted Si fragment, is significantly longer than that found in common η<sup>2</sup>-O<sub>2</sub> complexes, in which the sizes of the central atoms are nearly equal to that of Mo as a consequence of the strong trans influence of the silyl ligand. In contrast, the replacement of the phenyl group on a Si fragment by an electron-withdrawing perfluoro phenyl group, as in 3b, gives rise to a dramatic decrease in the trans influence. Treatment of 2a–c with 2 equiv of carboxylic acids, such as formic acid, acetic acid, and benzoic acid, readily leads to the formation of carboxylato molybdenum complexes, in which the carboxylate ligand coordinates to the metal in a monodentate mode. The resulting formato complex 4a1 can also be derived from the insertion of CO<sub>2</sub> into the Mo–H bond of 2a. In addition, complexes 2a,c,e mediate the catalytic carbon dioxide hydrogenation. The activity of the catalysts depends dramatically on the electronic effects of the substituents attached to the Si atom; electron-donating substituents lead to an increase in the catalytic activity. Reactions of complexes 2a,d with triflic acid yield highly labile triflate complexes, which can be further treated with aqueous NaOH to give hydroxo complexes 5a,d, respectively. The molecular structure of 5d has been determined by single-crystal X-ray diffraction. The reactivities of 2a–e are discussed in comparison with those of the parent complex [MoH<sub>4</sub>(dppe)<sub>2</sub>] (1; dppe = Ph<sub>2</sub>PCH<sub>2</sub>CH<sub>2</sub>PPh<sub>2</sub>).



## INTRODUCTION

Transition-metal complexes bearing silyl ligands continue to play an important role in organotransition-metal chemistry.<sup>1</sup> We previously reported the unexpected formation of novel molybdenum silyl hydrido complexes, [MoH<sub>3</sub>{[Ph<sub>2</sub>PCH<sub>2</sub>CH<sub>2</sub>P(Ph)C<sub>6</sub>H<sub>4</sub>-o]<sub>2</sub>(R)Si-P,P,P,P,Si}] (2a, R = Ph; 2b, R = C<sub>6</sub>F<sub>5</sub>; 2c, R = 4-Me<sub>2</sub>NC<sub>6</sub>H<sub>4</sub>; 2d, R = cyclohexyl; 2e, R = *n*-C<sub>6</sub>H<sub>13</sub>), with a pentadentate ligand composed of a P<sub>2</sub>SiP<sub>2</sub> framework, which can be readily made by the reaction of [MoH<sub>4</sub>(dppe)<sub>2</sub>] (1; dppe = Ph<sub>2</sub>PCH<sub>2</sub>CH<sub>2</sub>PPh<sub>2</sub>) with RSiH<sub>3</sub> in refluxing toluene (Scheme 1).<sup>2</sup> We found that this type of reaction was not limited to primary silanes. The reaction of PhGeH<sub>3</sub> with 1 afforded the related germyl

compound I. Even in the case of a secondary silane system, a similar reaction occurred to give the hydrido complex II with a tridentate ligand comprised of a P<sub>2</sub>Si framework (Chart 1).

Multidentate ligand systems containing Si as a donor atom have received increasing attention because the incorporation of a silyl group as part of the ligand framework could result in a number of unique properties for a metal.<sup>3,4</sup> These compounds are of interest for several reasons; among them, one is that silyl ligands are expected to exhibit an exceptionally strong trans effect due to their remarkable σ-donor and high trans-

Received: July 19, 2011

Published: July 9, 2012



Scheme 1

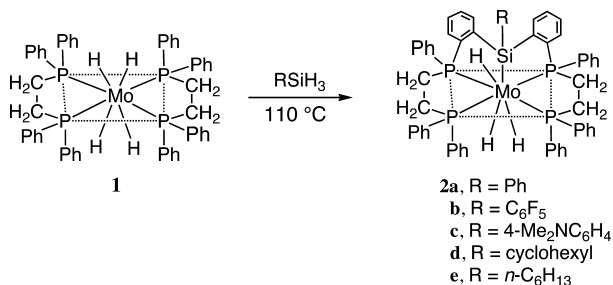
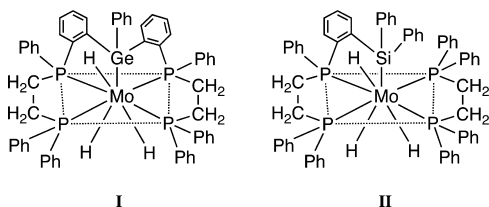


Chart 1



influencing ability.<sup>5</sup> In this context, we suspected that complexes **2a–e** may be excellent candidates for conducting a detailed investigation into the trans influence of silyl ligands. Indeed, the presence of the labile hydride ligands in the coordination sphere of molybdenum provides us with the ability to open up a site opposite to the Si atom, under mild conditions, for an incoming ligand via the reductive elimination of H<sub>2</sub>. Our recent work has demonstrated that complexes **2a–c** react rapidly with isocyanides to give isocyanido complexes in which the isocyanido group always ligates at the site opposite to the Si atom.<sup>6</sup> Furthermore, we have revealed that the trans-influencing ability imparted by the Si fragment in these isocyanido complexes is intimately dependent on the donor properties of the substituent attached to the Si atom.

In complexes **2a–e**, molybdenum atoms are presumably electron rich; therefore, their reactions with electrophiles may give products with intriguing structural features. We report, in the present contribution, the reactions of these complexes with electrophilic materials, including dioxygen, carbon dioxide, carboxylic acids, and triflic acid (CF<sub>3</sub>SO<sub>3</sub>H). Furthermore, their ability to act as a catalyst precursors for carbon dioxide fixation has been studied in detail. The preliminary results for some of the chemistry described herein have been previously communicated.<sup>2b,7</sup>

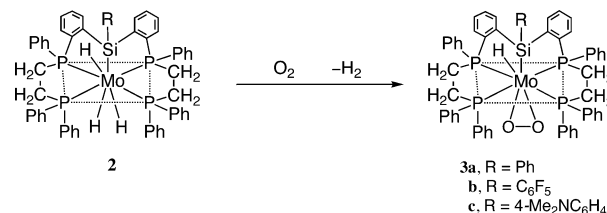
## RESULTS AND DISCUSSION

**Synthesis and Characterization of Dioxygen Complexes.** During our study of the chemical properties of **2a**, we found that a solution of **2a** is very susceptible to air and its color changes from yellow to green in the presence of even trace amounts of contaminated air. This observation suggested the formation of a dioxygen adduct of **2a**. Considerable attention has been focused on the interaction of dioxygen with transition-metal complexes, with particular reference to the activation of the former at the active center of a monooxygenase such as cytochrome P450. Previously, numerous dioxygen-coordinated transition-metal complexes have been reported.<sup>7</sup> Motivated by these facts, we set out to explore the reaction between **2a–c** and dioxygen.

Treating either THF or toluene solutions of the complexes with dioxygen (1 atm) at ambient temperature produced the

corresponding adducts (R = Ph (**3a**), C<sub>6</sub>F<sub>5</sub> (**3b**), 4-Me<sub>2</sub>NC<sub>6</sub>H<sub>4</sub> (**3c**)), which can be isolated as crystalline solids (Scheme 2). In

Scheme 2

Table 1. Preparation of ( $\eta^2$ -O) Complexes **3a–c**

compd	substrate complex (R)/amt, mmol	solvent/amt, mL	yield, %
3a	2a (Ph)/0.217	THF/22	87
3b	2b (C <sub>6</sub> F <sub>5</sub> )/0.092	toluene/10	89
3c	2c (4-Me <sub>2</sub> NC <sub>6</sub> H <sub>4</sub> )/0.096	toluene/10	82

Table 1, we summarize the reaction conditions. The evolution of a significant amount of dihydrogen was monitored using GLC when the reaction of **2a** with dioxygen was carried out in a sealed system.

Selected spectroscopic data for **3a–c** are compiled in Table 2. In the <sup>1</sup>H NMR spectra (C<sub>7</sub>D<sub>8</sub>), the hydride resonance for **3a**

Table 2. Selected Spectroscopic Data for **3a–c**

compd	IR $\nu$ (Mo–H), cm <sup>-1</sup>	<sup>1</sup> H NMR ( $J$ , Hz) <sup>a</sup>		<sup>31</sup> P NMR ( $J$ , Hz) <sup>a</sup>
		$\delta$ (Mo–H)	$\delta$ (other)	
3a	1708	0.10 (tt, 1H, $J_{PH}$ = 16, 40)	1.6–2.8 (m, 8H, C <sub>2</sub> H <sub>4</sub> ) 6.6–8.9 (m, 43H, Ph protons)	77 (d, 2P, $J_{PP}$ = 59) 105 (d, 2P, $J_{PP}$ = 59)
3b	1743	–0.05 (tt, 1H, $J_{PH}$ = 16, 39)	2.0–3.0 (m, 8H, C <sub>2</sub> H <sub>4</sub> ) 6.2–8.0 (m, 38H, Ph protons)	35 (br, 1P), 62 (br, 1P) 88 (br, 1P), 103 (br, 1P)
3c	1709	0.14 (tt, 1H, $J_{PH}$ = 16, 39)	2.2–2.5 (m, 8H, C <sub>2</sub> H <sub>4</sub> ) 2.62 (s, 6H, NCH <sub>3</sub> ) 6.0–8.0 (m, 42H, Ph protons)	35–65 (br, 2P) 90–100 (br, 2P)

<sup>a</sup>Measurements at room temperature.

is observed at  $\delta$  0.10 ppm (tt,  $^2J_{PH}$  = 16, 40 Hz), which is at a lower field than that for **2a** by about 4 ppm. This strong downfield shift could be interpreted as a consequence of the extremely electrophilic character of the dioxygen ligand. The hydride absorptions for **3b,c** are found to be close to that observed for **3a**. Apparently, the substituents attached to the Si atom have little influence on the electronic character of the metal center. The <sup>31</sup>P NMR spectra for **3a,c** at ambient temperature display two broad signals at low field ( $\delta$  105 ppm for **3a** and  $\delta$  95 ppm for **3c**) and at high field ( $\delta$  77 ppm for **3a** and  $\delta$  50 ppm for **3c**). In contrast, the spectrum for **3b** reveals four broad resonances at around 40, 60, 90, and 100 ppm. Cooling the solution of **3b** to –40 °C leads to the resolution of these peaks into four sharp doublets that are observed at  $\delta$  102 (d,  $^2J_{PP}$  = 44 Hz), 87 (d,  $^2J_{PP}$  = 212 Hz), 62 (d,  $^2J_{PP}$  = 44 Hz),

and 35 ppm ( $d$ ,  $^2J_{PP} = 212$  Hz) with a 1:1:1:1 peak area ratio, indicating the presence of four inequivalent P nuclei. This presumably occurs as a result of steric congestion at the Mo center; the Mo–O bond lengths in **3b** are significantly shorter than those observed in **3a** (vide infra).

The molecular structures of **3a,b**, as determined by X-ray crystallography are shown in Figures 1 and 2, with selected

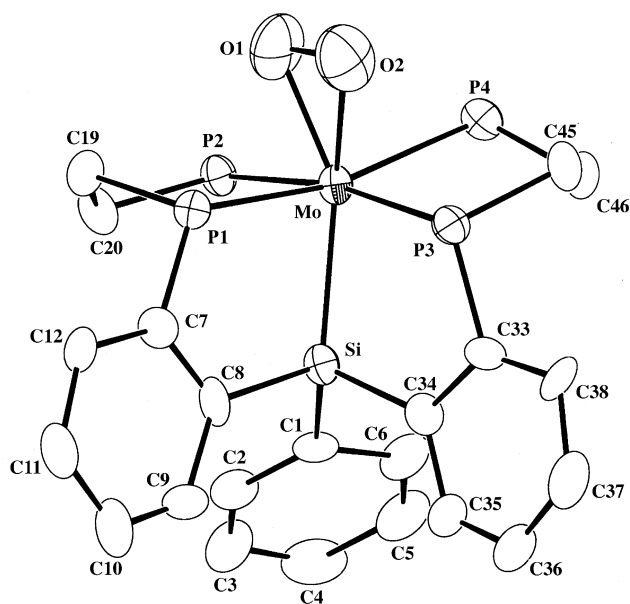


**Figure 1.** Molecular structure of **3a**. Phenyl rings that are not attached to the Si atom have been omitted for clarity. Selected bond distances (Å) and angles (deg): Mo–P1 = 2.434(5), Mo–P2 = 2.495(5), Mo–P3 = 2.422(5), Mo–P4 = 2.497(5), Mo–Si = 2.554(5), Si–C1 = 1.93(2), Si–C8 = 1.91(2), Si–C34 = 1.85(2), O1–O2 = 1.41(3), Mo–O1 = 2.12(1), Mo–O2 = 2.11(2); P1–Mo–P2 = 80.9(2), P2–Mo–P4 = 102.6(2), P1–Mo–P3 = 99.2(2), P3–Mo–P4 = 80.0(2), O1–Mo–O2 = 38.9(7), Mo–Si–C1 = 124.2(5), O1–Mo–Si = 144.9(5), O1–Mo–P2 = 74.2(5), O2–Mo–P1 = 83.9(5).

bond distances and angles given in the captions. Both complexes have similar structures and contain one dioxo ligand that is coordinated to the molybdenum atom in a side-on fashion. The two Mo–O bond lengths in **3a** (2.12(1) and 2.11(2) Å) are significantly longer than those found in common  $\eta^2$ -O<sub>2</sub> complexes in which the sizes of central atoms are nearly equal to that of Mo, e.g., [OsH( $\eta^2$ -O<sub>2</sub>)]{1,2-bis-(dicyclohexylphosphino)ethane}<sub>2</sub>]BPh<sub>4</sub> (2.045(8) and 2.037(8) Å)<sup>9</sup> and [CpW(O)( $\eta^2$ -O<sub>2</sub>)(CH<sub>2</sub>SiMe<sub>3</sub>)] (1.68(3) and 1.92(3) Å).<sup>10</sup> This feature may be attributed to the strong trans influence of the silyl ligand in **3a**. The observed O–O bond length is 1.41(3) Å; it is intermediate between those in peroxo (O<sub>2</sub><sup>2-</sup> = 1.49 Å) and superoxo groups (O<sub>2</sub><sup>-</sup> = 1.33 Å) and lies within the range reported for peroxo compounds (1.40–1.50 Å).<sup>11</sup>

A comparison of the metrical values for **3a,b** serves to elucidate the nature of the trans influence on these complexes. Figure 3 shows the experimental structural parameters for **3a,b**. The Mo–Si (2.546(2) Å) and Si–C(C<sub>6</sub>F<sub>5</sub> ring) (1.915(6) Å) distances and the Mo–Si–C(C<sub>6</sub>F<sub>5</sub> ring) angle (123.8(2)°) in **3b** are very close to the corresponding distances (2.554(5) and 1.93(2) Å) and angle (124.2(5)°) in **3a**. It may be inferred from these facts that **3a,b** are sterically very similar with respect to coordination, and therefore, the steric effects from the

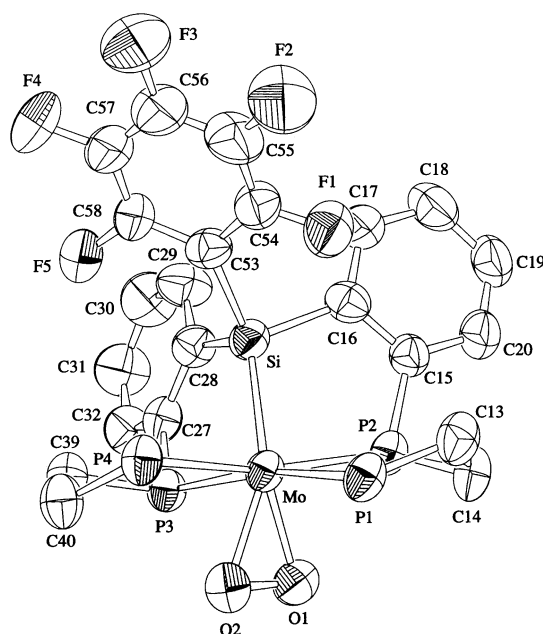


**Figure 2.** Molecular structure of **3b**. Phenyl rings that are not attached to the Si atom have been omitted for clarity. Selected bond distances (Å) and angles (deg): Mo–P1 = 2.536(2), Mo–P2 = 2.473(2), Mo–P3 = 2.470(1), Mo–P4 = 2.514(2), Mo–Si = 2.546(2), Si–C53 = 1.915(6), Si–C28 = 1.882(6), Si–C16 = 1.898(7), O1–O2 = 1.411(7), Mo–O1 = 2.051(4), Mo–O2 = 2.095(4); P1–Mo–P2 = 79.00(6), P2–Mo–P4 = 168.35(6), P1–Mo–P3 = 169.95(6), P3–Mo–P4 = 81.45(5), O1–Mo–O2 = 39.8(2), Mo–Si–C53 = 123.8(2), Mo–Si–C16 = 110.5(2), Mo–Si–C28 = 113.0(2), O1–Mo–O2 = 39.8(2), P2–Mo–O1 = 75.7(1), P1–Mo–O2 = 94.1(5).

substituents (C<sub>6</sub>H<sub>5</sub> and C<sub>6</sub>F<sub>5</sub>) on the nature of the Mo–O bond are rather weak. As a result, only the electronic effect will be at the origin of any variations in the measured parameters, and the amount of electron density of the Si atom will influence directly the interaction between the metal and the dioxo ligand.

Particularly noteworthy is the remarkable difference in the Mo–O bonds; the two Mo–O bond distances (mean 2.073 Å) in **3b** are significantly shorter than those in **3a** (mean 2.115 Å). This is the direct result of the electron-withdrawing C<sub>6</sub>F<sub>5</sub> group, which should reduce the  $\sigma$ -donor ability of the silyl ligand and strengthen the Mo–O linkages. In contrast, the O–O distances in the two compounds differ surprisingly little (1.41(3) Å for **3a**; 1.411(7) Å for **3b**). In general, in peroxo compounds, a  $\sigma$  bond is formed by filled O( $p\pi$ ) $\rightarrow$ M( $d\sigma$ ) bonding and back-bonding is due to M( $d\pi$ ) $\rightarrow$ O( $\pi^*$ ).<sup>11</sup> Taking into account these facts, we can conclude that the presence of an electron-withdrawing group on the silyl ligand reduces the  $\pi$ -back-donation ability of the molybdenum fragment.

Treatment of the parent complex **I** or the molybdenum silyl complex **II** with dioxo in solution, only resulted in the deterioration of the starting complex, indicating that the structural rigidity imposed by the pentadentate framework in **3a–c** is crucial in stabilizing peroxo-type dioxo complexes of Mo(IV).

**Synthesis and Characterization of Monocarboxylato Complexes.** Complexes **2a–c** react with 2 equiv of carboxylic acids such as formic acid, acetic acid, and benzoic acid at room temperature to give the monocarboxylato compounds **4a1–c3** in good yields (70–90%, Scheme 3). In Table 3, we summarize the reaction conditions.

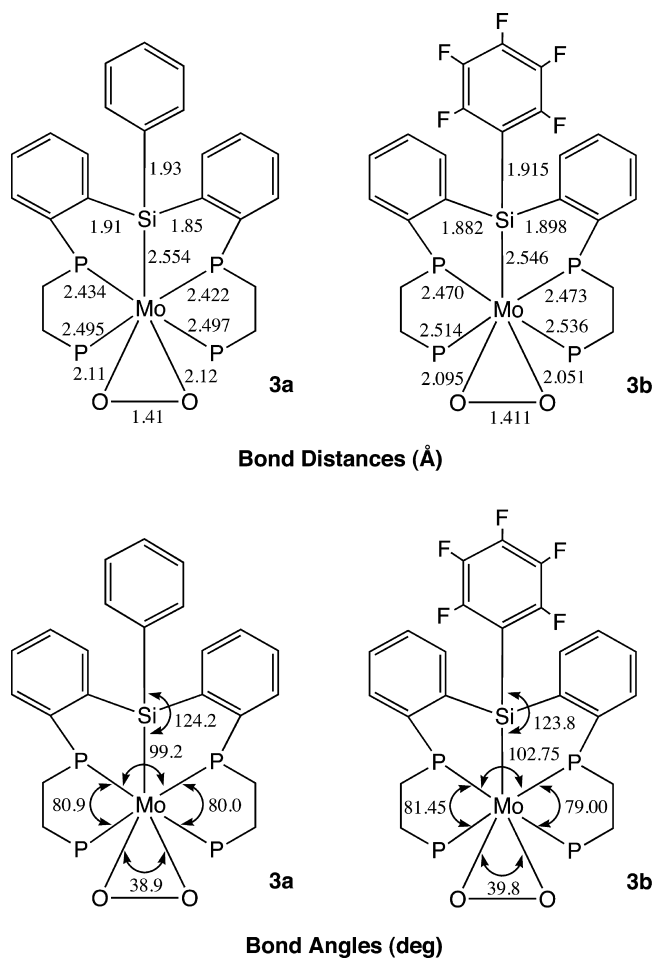


Figure 3. Experimental structures for 3a,b with selected structural parameters.

### Scheme 3

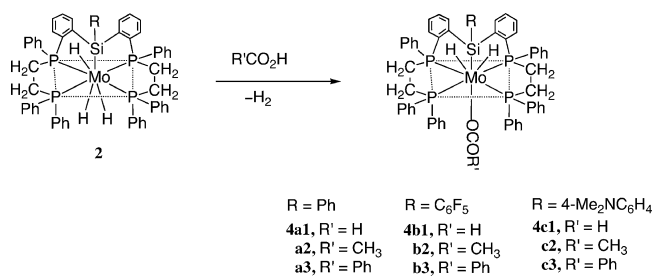


Table 3. Preparation of Monocarboxylato Complexes

compd	substrate		yield, %
	complex (R)/amt, mmol	acid/amt, mmol	
4a1	2a (Ph)/0.162	HCOOH/0.325	7
4a2	2a (Ph)/0.268	CH <sub>3</sub> COOH/0.536	90
4a3	2a (Ph)/0.234	PhCOOH/0.468	87
4b1	2b (C <sub>6</sub> F <sub>5</sub> )/0.092	HCOOH/0.180	12
4b2	2b (C <sub>6</sub> F <sub>5</sub> )/0.092	CH <sub>3</sub> COOH/0.210	82
4b3	2b (C <sub>6</sub> F <sub>5</sub> )/0.092	PhCOOH/0.210	90
4c1	2c (4-Me <sub>2</sub> NC <sub>6</sub> H <sub>4</sub> )/0.096	HCOOH/0.960	16
4c2	2c (4-Me <sub>2</sub> NC <sub>6</sub> H <sub>4</sub> )/0.096	CH <sub>3</sub> COOH/0.960	69
4c3	2c (4-Me <sub>2</sub> NC <sub>6</sub> H <sub>4</sub> )/0.096	PhCOOH/0.290	55

During the reactions, the evolution of the hydrogen gas was qualitatively monitored by GLC analysis. Selected NMR spectroscopic data for the resulting complexes are compiled in Table 4. In the <sup>1</sup>H NMR spectra for 4a1–c3, hydrido signals

Table 4. Selected NMR Spectroscopic Data for 4a1–c3

compd	<sup>1</sup> H NMR (J, Hz) <sup>a</sup>		<sup>31</sup> P NMR (J, Hz) <sup>a</sup>
	δ(Mo–H)	δ(other)	
4a1	−8.01 (tt, 2H, J <sub>PH</sub> = 17, 43)	1.9–3.0 (m, 8H, C <sub>2</sub> H <sub>4</sub> )	59 (br d, 2P, J <sub>PP</sub> = 122)
		6.1–8.9 (m, 43H, Ph protons)	88 (br d, 2P, J <sub>PP</sub> = 122)
4a2	−7.96 (tt, 2H, J <sub>PH</sub> = 17, 43)	1.23 (s, CH <sub>3</sub> CO), 2.0–3.0 (m, 8H, C <sub>2</sub> H <sub>4</sub> )	59 (br d, 2P, J <sub>PP</sub> = 122)
		6.2–8.9 (m, 43H, Ph protons)	88 (br d, 2P, J <sub>PP</sub> = 122)
4a3	−7.92 (tt, 2H, J <sub>PH</sub> = 17, 43)	1.9–3.0 (m, 8H, C <sub>2</sub> H <sub>4</sub> )	59 (br d, 2P, J <sub>PP</sub> = 121)
		6.0–8.9 (m, 48H, Ph protons)	87 (br d, 2P, J <sub>PP</sub> = 119)
4b1	−8.10 (tt, 2H, J <sub>PH</sub> = 18, 43)	1.8–3.2 (m, 8H, C <sub>2</sub> H <sub>4</sub> )	55 (br d, 2P, J <sub>PP</sub> = 119)
		6.0–8.0 (m, 38H, Ph protons)	87 (br d, 2P, J <sub>PP</sub> = 119)
4b2	−8.00 (tt, 2H, J <sub>PH</sub> = 18, 43)	1.10 (s, CH <sub>3</sub> CO), 1.8–3.2 (m, 8H, C <sub>2</sub> H <sub>4</sub> )	55 (br d, 2P, J <sub>PP</sub> = 122)
		6.3–8.0 (m, 38H, Ph protons)	87 (br d, 2P, J <sub>PP</sub> = 122)
4b3	−8.00 (tt, 2H, J <sub>PH</sub> = 18, 43)	2.0–3.4 (m, 8H, C <sub>2</sub> H <sub>4</sub> )	55 (br d, 2P, J <sub>PP</sub> = 119)
		6.3–8.2 (m, 43H, Ph protons)	86 (br d, 2P, J <sub>PP</sub> = 119)
4c1	−8.10 (tt, 2H, J <sub>PH</sub> = 17, 43)	2.2–2.6 (m, 8H, C <sub>2</sub> H <sub>4</sub> ), 2.73 (s, 6H, NCH <sub>3</sub> )	59 (br d, 2P, J <sub>PP</sub> = 121)
		6.0–8.3 (m, 42H, Ph protons)	87 (br d, 2P, J <sub>PP</sub> = 121)
4c2	−7.90 (tt, 2H, J <sub>PH</sub> = 17, 44)	1.70 (s, CH <sub>3</sub> CO), 2.1–2.7 (m, 8H, C <sub>2</sub> H <sub>4</sub> )	60 (br d, 2P, J <sub>PP</sub> = 122)
		2.73 (s, 6H, NCH <sub>3</sub> ), 6.0–8.5 (m, 42H, Ph protons)	88 (br d, 2P, J <sub>PP</sub> = 122)
4c3	−7.90 (tt, 2H, J <sub>PH</sub> = 17, 44)	2.3–2.7 (m, 8H, C <sub>2</sub> H <sub>4</sub> ), 2.75 (s, 6H, NCH <sub>3</sub> )	59 (br d, 2P, J <sub>PP</sub> = 119)
		6.0–8.3 (m, 47H, Ph protons)	88 (br d, 2P, J <sub>PP</sub> = 119)

<sup>a</sup>Measurement at room temperature.

appeared at around δ −8 as a triplet of triplets, corresponding to an A<sub>2</sub>K<sub>2</sub>X spin system. The <sup>31</sup>P{<sup>1</sup>H} NMR spectra for 4a1–c3 appear as a typical AX system with two doublets. The presence of only two resonances indicates that they have an effective mirror plane containing the Mo–Si bond. The IR spectra for complexes 4a1–c3 showed two ν(OCO) stretching frequencies (asym and sym) near 1600 and 1330 cm<sup>−1</sup>, respectively (Table 5). The fairly large values of Δν (ν(OCO)<sub>asym</sub> − ν(OCO)<sub>sym</sub>), ranging from 239 to 329 cm<sup>−1</sup>, suggest that the carboxylate ligands in these complexes coordinate to molybdenum in a monodentate fashion, as shown in Scheme 3.<sup>12</sup>

The basic features of the structure of these complexes deduced from the spectra were fully confirmed by the single-crystal X-ray diffraction analysis of 4a2. A representation of the molecule of 4a2 is shown in Figure 4, with selected bond distances and angles given in the caption.

As expected from the aforementioned IR and NMR results, this complex contains a pentadentate P<sub>2</sub>SiP<sub>2</sub> ligand and a monodentate acetate ligand. If the hydrido ligands are ignored,

Table 5. Carboxyl Stretching Frequencies ( $\text{cm}^{-1}$ ) of 4a1–c3

compd	$\nu(\text{C}=\text{O})_{\text{asym}}$	$\nu(\text{C}-\text{O})_{\text{sym}}$	$\Delta^a$
4a1	1618	1325	293
4a2	1617	1338	279
4a3	1609	1330	279
4b1	1624	1311	313
4b2	1639	1310	329
4b3	1622	1311	311
4c1	1596	1351	245
4c2	1596	1357	239
4c3	1696	1356	240

<sup>a</sup>Difference between two frequencies.

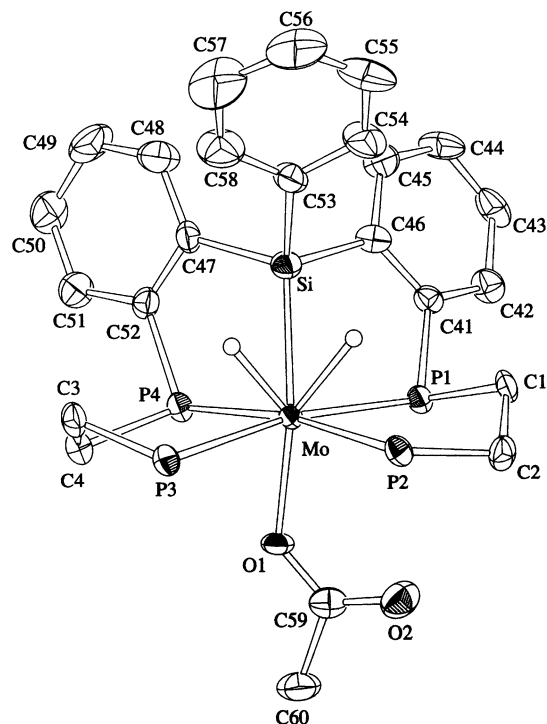


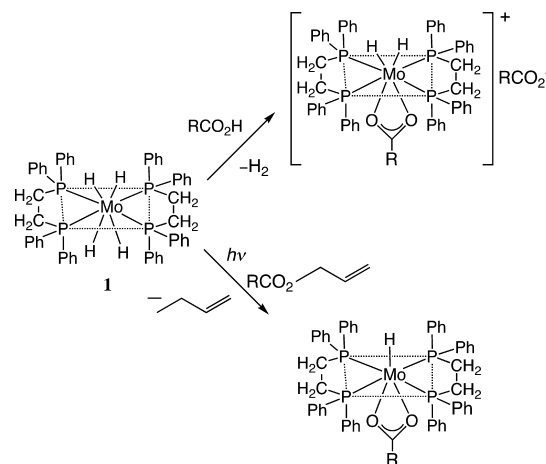
**Figure 4.** Molecular structure of 4a2. Phenyl rings that are not attached to the Si atom have been omitted for clarity. Selected bond distances (Å) and angles (deg): Mo–P1 = 2.485(2), Mo–P2 = 2.507(2), Mo–P3 = 2.496(2), Mo–P4 = 2.466(2), Mo–Si = 2.515(2), Si–C46 = 1.911(7), Si–C47 = 1.887(7), Si–C53 = 1.869(8), Mo–O1 = 2.174(5), O1–C59 = 1.239(9), O2–C59 = 1.219(10); P1–Mo–P2 = 80.31(6), P2–Mo–P3 = 96.32(6), P3–Mo–P4 = 80.16(2), P1–Mo–P4 = 101.77(2), Si–Mo–O1 = 143.7(1), Mo–Si–C47 = 113.2(2), Mo–Si–C53 = 122.7(2), Mo–Si–C46 = 111.0(2), Mo–O1–C59 = 130.8(5), O2–C59–C60 = 117.4(8), O1–C59–O2 = 125.1(8).

the geometry of the Mo center is a distorted octahedron. The equatorial plane is defined by Mo1, P1, P2, P3, and P4 ( $\sum(\text{X}-\text{Mo}-\text{Y}) = 358.56^\circ$ ), and Si and O1 occupy the pseudoaxial positions ( $\text{O}-\text{Mo}-\text{Si} = 143.7(1)^\circ$ ).

In our previous work, we showed that the parent complex **1** reacted with carboxylic acids to give cationic carboxylato complexes in which the carboxylato is bound as a bidentate ligand (Scheme 4).<sup>13</sup> Furthermore, **1** reacted with allyl carboxylate upon irradiation, giving exclusively a chelating complex.<sup>14</sup>

Therefore, the most interesting feature of the structure is the monodentate mode observed for the carboxylate ligands in 4a1–c3. At first sight, the restricted geometric arrangement in

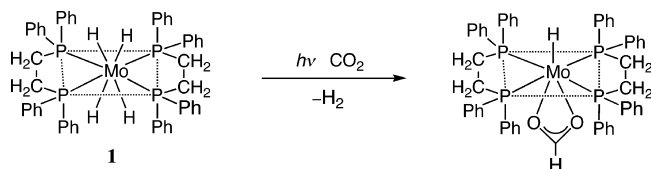
Scheme 4



2a–c appears to prevent chelate formation. However, in our recent studies, we showed that **2a** reacts with 2,4-pentanedione to give a dihydrido complex with a chelating 2,4-pentanedionate ligand, which results from the repulsion of one of the four Mo–P bonds in the  $\text{P}_2\text{SiP}_2$  ligand.<sup>15</sup> Hence, we believe that in 2a–c the simultaneous availability of two vacant coordination sites on the metal center is not unlikely. The acetate ligand probably does not have a sufficiently strong  $\pi$ -donor character in the present system.

**Reaction of Complex 2a with Carbon Dioxide.** The formation of formato complexes 4a1, 4b1, and 4c1 led us to study the reactivity of **2a** toward carbon dioxide, since reactions of a number of transition-metal hydrido complexes with carbon dioxide yield formato complexes resulting from the insertion reaction of carbon dioxide into M–H bonds.<sup>16</sup> For example, experiments in our laboratory allowed us to establish that the irradiation of a benzene solution of **1** under a carbon dioxide atmosphere yields a chelating formato- $\text{O},\text{O}'$  complex (Scheme 5).<sup>17</sup>

Scheme 5

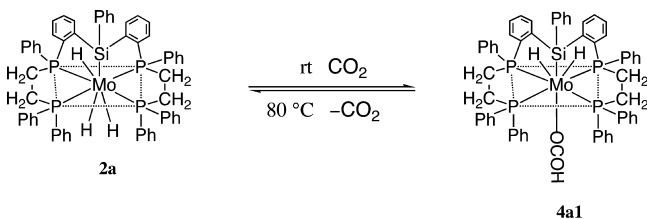


A toluene solution of complex **2a** was allowed to react under  $\text{CO}_2$  pressure (17 atm) at room temperature, and the expected formato complex 4a1 was isolated in 82% yield from the reaction mixture. In addition, an NMR study provided evidence that 4a1 loses  $\text{CO}_2$  fairly easily, regenerating **2a** at 80 °C in benzene (Scheme 6).

The insertion reaction of carbon dioxide into a Mo–H bond under mild conditions is an outstanding feature exhibited by complex **2a**, since the parent complex **1** does not react with carbon dioxide at ambient temperature. As described above, the reaction between **1** and carbon dioxide requires forcing conditions to proceed to completion. Thus, the marked difference in their reactivities underscores the strong trans-influencing ability of the Si fragment.

**Catalytic Hydrogenation of Carbon Dioxide.** In view of the straightforward insertion mode of  $\text{CO}_2$  into the Mo–H

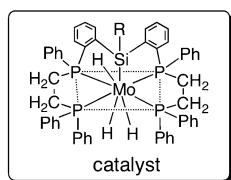
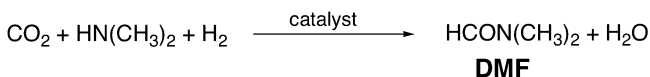
Scheme 6



bond of **2a**, we decided to investigate the capability of **2a** to catalyze the hydrogenation of  $\text{CO}_2$  itself. Many studies have previously shown that metal formate complexes are assumed to be the active catalytic intermediates in this process.<sup>18</sup>

The catalytic reactions were performed at  $110\text{ }^\circ\text{C}$  in a stainless-steel autoclave under  $\text{CO}_2/\text{H}_2$  gas mixtures in the presence of dimethylamine to provide *N,N*-dimethylformamide (DMF). The results of the hydrogenation of  $\text{CO}_2$  using **2a–c,e** are summarized in Table 6. Additionally, in order to compare

**Table 6.** Effect of Catalyst on TON of Hydrogenation of  $\text{CO}_3^a$



entry no.	cat. (R)	TON <sup>b</sup>
1	<b>2a</b> (Ph)	92
2	<b>2b</b> ( $\text{C}_6\text{F}_5$ )	1
3	<b>2c</b> (4- $\text{Me}_2\text{NC}_6\text{H}_4$ )	130
4	<b>2e</b> ( <i>n</i> - $\text{C}_6\text{H}_{13}$ )	110
5	<b>I</b>	0
6	<b>I<sup>c</sup></b>	0
7	<b>II<sup>c</sup></b>	9

<sup>a</sup>Conditions:  $110\text{ }^\circ\text{C}$ , 20–25 atm of  $\text{CO}_2$ , 30–40 atm of  $\text{H}_2$ , 50 mmol of  $\text{HN}(\text{CH}_3)_2$  (25 mL, 2.0 M solution in toluene), 0.2 mmol of catalyst. <sup>b</sup>TON = turnover number = mol of product (DMF)/mol of catalyst. <sup>c</sup>See Chart 1.

the effects of the Si ligand system on the catalytic reactivity, parent complex **I**, germanium congener **I**, and complex **II** containing a tridentate ligand were included in this study. The results are summarized in Table 6.

As can be seen from the table, there is a wide range of values obtained for the catalytic activity. Complex **2c** is the most active; the use of **2c** allows the reaction to reach a turnover number (TON) of 130. The presence of electron-donating substituents on the Si ligand in this catalyst system may lead to an increase in catalytic activity, because complexes **2c,e** are more reactive than complex **2a**. Furthermore, this increase seems to parallel the increase in electron density of the Si atom. Consistent with this premise, no catalytic reaction was found with **2b**. The electron-withdrawing substituent dramatically suppresses the activity. Interestingly, complex **II** is much less active than complex **2a**. Moreover, as can be appreciated from the table, both complexes **I** and **I** are virtually inactive. These results strongly suggest that both the Mo–Si linkage and the

$\text{P}_2\text{SiP}_2$  girdle in complexes **2a,c,e** play an important role in the present catalytic process.

A possible mechanism for the catalytic formation of DMF should have three steps. The initial step is the hydrogenation of  $\text{CO}_2$  to formic acid. The resulting formic acid reacts with dimethylamine to yield ammonium formate, followed by dehydration. Thermal condensation of dimethylamine and formic acid is known to proceed at  $100\text{ }^\circ\text{C}$ ;<sup>19</sup> hence, the dehydration is easily performed in our process.

Alternative pathways for the formation of formic acid catalyzed by transition-metal hydrido complexes ( $\text{L}_n\text{M–H}$ ) have been proposed on the basis of some experimental evidence and theoretical calculations, as outlined in Scheme 7.<sup>20</sup> Path A (the classical process) involves  $\text{CO}_2$  insertion into a M–H bond, followed by a sequence of oxidative addition and reductive elimination steps for the  $\text{H}_2$  activation process.

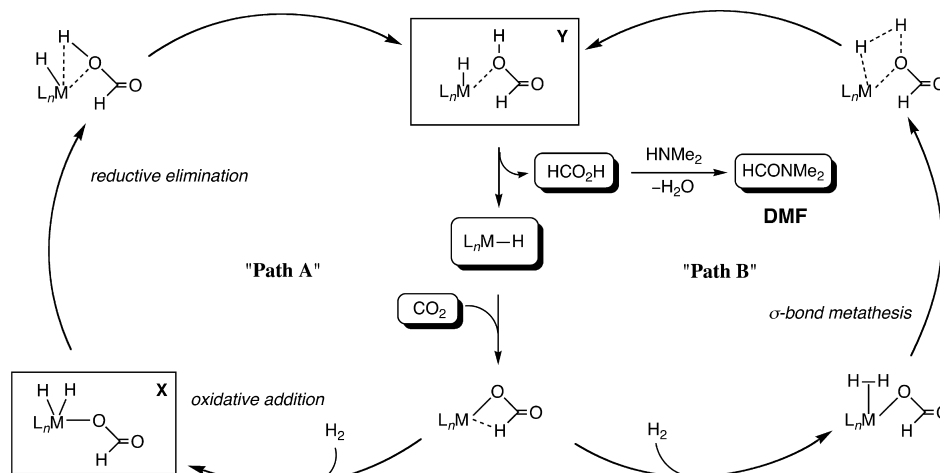
However, Dedieu et al. have recently suggested a different pathway ( $\sigma$ -bond metathesis) in which no change in the oxidation state of the metal center is required and the formation of formic acid is a result of a  $[2 + 2]$  addition of  $\text{H}_2$  on a metal formate intermediate obtained after  $\text{CO}_2$  insertion (path B of Scheme 7).<sup>21</sup> The present catalytic process can be explained by either path A or path B.

Dedieu et al. established that the reductive elimination of formic acid from an intermediate formate hydrido complex **X** is the rate-limiting step for path A, whereas the liberation of formic acid from a formic acid complex **Y** is the rate-limiting step for path B.<sup>21</sup> Our study has shown that the thermolysis of formate hydrido complex **4a1** leads only to the evolution of  $\text{CO}_2$  and regeneration of **2a**; therefore, complex **4a1** does not reductively eliminate formic acid (Scheme 6). Thus, we believe that a  $\sigma$ -bond metathesis reaction occurs in the present process. Although we must await further investigations to elucidate the correct mechanism of our process, we can consider the present experimental results useful because the trans effect of the silyl ligand can efficiently operate in both these pathways. As discussed in the previous section, the studies performed on the dioxygen complexes have shown that the perfluoro phenyl group in **3b** decreases substantially the trans influence properties of the Si ligand and causes a dramatic strengthening of the Mo–O linkages. Accordingly, it seems likely that both the reductive elimination of formic acid and the liberation of formic acid do not occur easily in intermediate complexes derived from **2b**. In direct contrast to **2b**, the incorporation of a  $\text{Me}_2\text{N}$  group at the 4-position of Ph is expected to elicit the opposite effect; hence, this leads to **2c** being the most efficient catalyst precursor.

**Reactions of 2a,d with Triflic Acid.** The reactions of **2a–c** with relatively weak acids, i.e., carboxylic acids, were observed to result in the formation of monocarboxylato molybdenum complexes. Subsequently, we focused on the further reaction chemistry of them with strongly acidic  $\text{CF}_3\text{SO}_3\text{H}$  (triflic acid, TfOH).

Reactions of metal alkyl and hydrido complexes with strong protonic acids, such as triflic acid, have provided a general synthetic route to metal complexes with weakly coordinated ligands.<sup>22</sup> Furthermore, in the case of **2a**, there is a possibility of breakage of the silyl ligand, since the reaction of  $\text{PhSiH}_3$  with triflic acid results in the preferential cleavage of the Si–Ph bond, generating  $\text{H}_3\text{SiOTf}$  and benzene.<sup>23</sup> This process has proved to be a very simple, energetically accessible reaction. Consequently, it seems to be difficult to make reliable

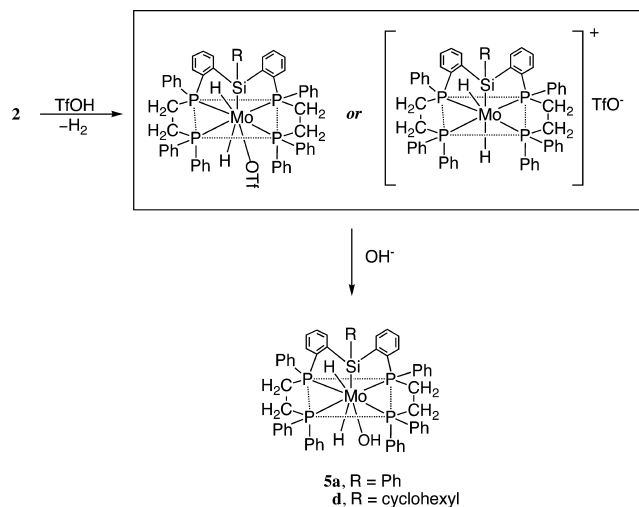
Scheme 7



predictions for the final products of the reaction between **2a** and triflic acid.

The treatment of a brown THF solution of complex **2a** with 1.2 equiv of triflic acid at  $-78\text{ }^{\circ}\text{C}$  resulted in an obvious color change to red, but the resulting products were not sufficiently stable under these conditions and attempts to isolate the products were unsuccessful. Thus, the desired products were converted into the more stable hydroxide complex **5a** on treatment with aqueous NaOH (Scheme 8). The cyclohexyl analogue **5d** can be prepared in a similar manner.

Scheme 8



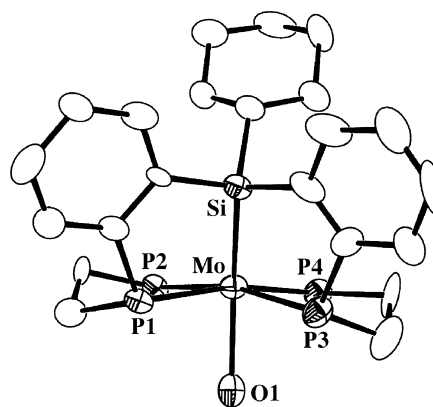
Selected spectroscopic data for **5a,d** are compiled in Table 7. IR absorptions near  $1820$  and  $3460\text{ cm}^{-1}$  are respectively attributable to  $\nu(\text{Mo}-\text{H})$  and  $\nu(\text{Mo}-\text{OH})$ . In the  $^1\text{H}$  NMR spectra, hydrido signals appeared at around  $\delta -7.5$  as a triplet of triplets corresponding to an  $A_2K_2X$  spin system. The  $^{31}\text{P}\{^1\text{H}\}$  NMR spectra for these complexes appear as a typical AX system with two doublets. The presence of only two resonances indicates that the molecules have an effective mirror plane containing a Mo-Si bond. The features of the NMR spectra for **5a,d** are very similar to those for the above monocarboxylato complexes, suggesting that these complexes have analogous structures.

Table 7. Selected Structural Data for **5a,d**

compd	IR/ $\text{cm}^{-1}$		$^1\text{H}$ NMR (J, Hz) <sup>a</sup>		$^{31}\text{P}$ NMR (J, Hz) <sup>a</sup>
	$\nu(\text{Mo}-\text{H})$	$\nu(\text{Mo}-\text{OH})$	$\delta(\text{Mo}-\text{H})$	$\delta(\text{other})$	
<b>5a</b>	1810	3452	$-7.25$ (tt, 2H, $J_{\text{HP}} = 16, 46$ )	$2.0-2.8$ (m, 8H, $\text{C}_2\text{H}_4$ )	54 (d, 2P, $J_{\text{PP}} = 144$ ) 88 (d, 2P, $J_{\text{PP}} = 144$ )
<b>5d</b>	1825	3484	$-7.59$ (tt, 2H, $J_{\text{HP}} = 16, 46$ )	$1.6-2.8$ (m, 8H, $\text{C}_2\text{H}_4$ )	51 (d, 2P, $J_{\text{PP}} = 141$ ) 89 (d, 2P, $J_{\text{PP}} = 141$ )

<sup>a</sup>Measurement at room temperature.

Crystals of **5d** were grown from solution in a benzene/hexane solvent mixture at  $0\text{ }^{\circ}\text{C}$ , and the molecular structure of **5d** was confirmed by a single-crystal X-ray diffraction study. A molecular structure of **5d** is shown in Figure 5, with selected bond distances and angles given in the caption. We note that the accuracy of these metrical parameters is not completely



**Figure 5.** Molecular structure of **5d**. Phenyl rings that are not attached to the Si atom have been omitted for clarity. Selected bond distances ( $\text{\AA}$ ) and angles (deg): Mo-P1 =  $2.462(3)$ , Mo-P2 =  $2.486(5)$ , Mo-P3 =  $2.475(4)$ , Mo-P4 =  $2.510(4)$ , Mo-Si =  $2.519(4)$ , Si-C7 =  $1.922(17)$ , Si-C1 =  $1.884(13)$ , Si-C33 =  $1.903(16)$ , Mo-O1 =  $2.258(9)$ ; P1-Mo-P2 =  $81.31(15)$ , P1-Mo-P3 =  $98.84(15)$ , P3-Mo-P4 =  $80.26(14)$ , P2-Mo-P4 =  $97.29(15)$ , Si-Mo-O1 =  $147.44(2)$ , Mo-Si-C7 =  $110.81(5)$ , Mo-Si-C1 =  $125.79(5)$ , and Mo-Si-C33 =  $109.23(4)$ .

satisfactory. The crystal of **5d** was not good enough for refinement ( $R = 0.1330$ ), and this problem prevented a high-quality structure determination. However, the substituents are rather well-defined and have their expected geometries.

If the hydrido ligands are ignored, the coordination geometry around the Mo center is a distorted octahedron. The equatorial plane is defined by Mo1, P1, P2, P3, and P4; Si and O occupy the pseudoaxial positions. The Mo–O separation of 2.258(9) Å in **5d** is much longer than the typical value for an M=O bond in oxo compounds ( $\sim 1.59\text{--}1.66$  Å).<sup>24</sup> Furthermore, this Mo–O bond length is comparable with the value of 2.174(5) Å in **4a2**. These observations strongly suggest a single bond between molybdenum and oxygen. Thus, the oxygen atom, O1, is actually a hydroxide, OH. Indeed, the IR spectra for **5a,d** were consistent with the presence of a characteristic O–H stretching frequency between 3452 (**5a**) and 3484  $\text{cm}^{-1}$  (**5d**) (vide supra).

As mentioned previously, the reactions between triflic acid and complex **2a** may proceed by two pathways to give the main products including (a) protonation at the molybdenum atom and (b) cleavage of the Si–Ph bond. Our results have shown that the end product corresponds structurally to the hydroxide coordination adduct, and hence, the initial stage of this reaction would be protonation at the metal center to give a triflate complex.

We note here that a similar reaction of **2a** with trifluoroacetic acid, followed by treatment with aqueous NaOH, led exclusively to an  $\eta^1\text{-O}_2\text{CCF}_3$  complex, while complex **5a** was not able to be detected.<sup>25</sup> Perhaps this is not surprising, given that the triflate complex possesses a greatly enhanced reactivity in comparison with the  $\eta^1\text{-O}_2\text{CCF}_3$  complex. Thus, the triflate precursor is an attractive candidate for preparing novel types of complexes bearing polydentate phosphinoalkyl–silyl ligands. Transition-metal complexes containing a triflate ligand have been studied extensively because they may be versatile and important reagents in mechanistic studies and organometallic synthesis. Efforts in this direction are continuing.

In addition, hydroxide complexes are interesting in their own right, since they are central to catalytic reactions such as the Wacker process and the water-gas shift reaction. Consequently, further studies investigating the catalytic performance of these complexes are in progress.

## CONCLUSIONS

Several important conclusions can be made from our results. Complexes **2a–e** are found to exhibit significant differences in their reactions with electrophilic materials in comparison to the parent complex  $[\text{MoH}_4(\text{dppe})_2]$  (**1**). These differences are interpreted in terms of a combination of the strong trans-labilizing ability of the Si group and the unusual quintuply chelated structure of these complexes. Unlike **1**, which decomposes in the presence of dioxygen, stable  $\eta^2\text{-O}_2$  complexes **3a–c** are formed by the reactions of **2a–c** with dioxygen. The treatment of **2a–c** with carboxylic acids gives neutral molybdenum complexes **4a1–c3** with a monodentate carboxylate ligand, while the analogous reaction with **1** leads to a cationic carboxylato complex possessing a chelating bidentate structure. Carbon dioxide reacts reversibly with **2a** at room temperature to form formate complex **4a1**, which is also obtained by the reaction of **2a** with formic acid. In the case of **1**, this similar reaction does not occur. Furthermore, we have found that DMF is prepared by the catalytic hydrogenation of carbon dioxide under pressure at 110 °C in the presence of

dimethylamine and **2a**. In contrast, when the experiment is performed under identical conditions in the presence of **1** as a catalyst there is no measurable formation of DMF. To our knowledge, complex **2a** is the first example of a molybdenum phosphine compound that has proved to be a considerably efficient catalyst for a carbon dioxide fixation reaction. In summary, the introduction of the silyl group into the dppe ligand system dramatically changes the reactivity of the molybdenum polyhydrido complexes and remarkably enhances their catalytic performance. Additionally, we investigated the influence of different substituents, directly attached to the Si atom of the silyl ligand, on their chemical behavior. We have revealed that electron-donating substituents increase the trans-influencing ability of the Si group and lead to an increase in the catalytic activity.

Owing to their important role in several metal-catalyzed processes, including olefin hydrosilylation, silane alcoholysis, and dehydropolymerization of silanes, transition-metal silyl complexes have received a great deal of attention. The present investigations of the reactivities of **2a–e** suggest that transition-metal silyl complexes deserve considerable interest with respect to other catalytic processes. The new complexes reported here provide us with the basis for further development of the chemistry of transition-metal silicon complexes in the areas of small-molecule activation and catalysis.

## EXPERIMENTAL SECTION

**General Procedures.** All manipulations were performed using standard Schlenk techniques under purified argon. All reagents were purchased from commercial suppliers and used as received without further purification. All solvents were dried by standard methods and were stored under argon. Complexes **2a–e** were synthesized according to procedures previously reported.<sup>2</sup> NMR data were recorded on either a JEOL-JNM-EX270 or a JEOL-JNM-AL400 instrument. <sup>31</sup>P{<sup>1</sup>H} NMR peak positions were referenced to external PPh<sub>3</sub>.

**Synthesis and Characterization of Dioxygen Complexes.** A pale yellow solution of **2a** (217 mg, 0.217 mmol) in dry THF (22 mL) turned green on exposure to 1 atm of dioxygen with stirring for 2 h at ambient temperature. After evaporation of the solvent under vacuum, the residue was washed with hexane and then recrystallized from THF/hexane to afford **3a** (213 mg, 87%) of greenish crystals. Anal. Calcd for C<sub>66</sub>H<sub>68</sub>MoO<sub>4</sub>P<sub>4</sub>Si (**3a**·2THF): C, 67.57; H, 5.84. Found: C, 67.24; H, 5.16. This procedure is also applicable to the synthesis of the other dioxygen complexes (**3b,c**). Experiments given in Table 1 were carried out under essentially the same conditions. Spectral data for **3a–c** are summarized in Table 2. Satisfactory microanalytical data for **3b,c** were not obtained after several attempts.

**Synthesis and Characterization of Monocarboxylato Complexes.** To a stirred solution of **2b** (100 mg, 0.092 mmol) in dry toluene (10 mL) was added glacial acetic acid (11.8  $\mu\text{L}$ , 0.210 mmol) drop by drop with a syringe at ambient temperature. After further stirring for 10 h, the color of the mixture changed from yellow to orange. Addition of excess hexane to the resulting mixture gave a yellow precipitate. After removal of the supernatant, the precipitate was dried under reduced pressure and then washed with hexane. The resulting solid was dried in vacuo to give **4b2** (85 mg, 82%). This procedure is also applicable to the synthesis of the other monocarboxylato complexes. Experiments given in Table 3 were carried out under essentially the same conditions. Spectral data for **4a1–c3** are summarized in Table 4. Brown crystals of **4a2**, suitable for an X-ray structure determination, were grown from THF/hexane solution at  $-10$  °C. Complexes **4a1–c3** were too unstable to allow satisfactory elemental analyses. Repeated purifications by recrystallization or reprecipitating led to partial decomposition with concomitant formation of small amounts of impurities.

**Reaction of Complex 2a with Carbon Dioxide.** **2a** (310 mg, 0.310 mmol) was dissolved in dry THF (35 mL) in a Schlenk flask

under an argon atmosphere. The solution was transferred into an autoclave equipped with a stir bar. The autoclave was then pressurized to 19 atm with CO<sub>2</sub> and was stirred at ambient temperature for 3 h. The reactor was vented at ambient temperature, and the reaction mixture was transferred into a Schlenk flask under an argon atmosphere. Hexane (15 mL) was then added, and the mixture was allowed to stand for 12 h at 0 °C, whereupon a yellow precipitate separated out. The product was collected by filtration, washed with hexane (10 mL × 2), and then dried in vacuo to give a yellow solid, which was identified as **4a1** (265 mg, 82%) on the basis of its spectroscopic properties.

**Catalytic Hydrogenation of Carbon Dioxide.** In a typical experiment, a catalyst (0.2 mmol) and dimethylamine (25 mL, 50 mmol, 2.0 M solution in toluene) were combined in a Schlenk flask under an argon atmosphere. Then, the solution was transferred into an autoclave equipped with a stir bar. The autoclave was sealed, pressurized to 50 atm with CO<sub>2</sub>/H<sub>2</sub> (3/2), and heated to 110 °C. After 24 h of stirring, the autoclave was vented and the reaction mixture was transferred into a Schlenk flask. The volatiles were vacuum-transferred into another vessel and then analyzed by GLC. Yields of DMF obtained were determined relative to an internal mesitylene standard. The results are collected in Table 6.

**Reaction of 2a,d with Triflic Acid.** To a stirred solution of **2d** (280 mg, 0.280 mmol) in dry THF (32 mL) was added neat triflic acid (0.030 mL, 0.34 mmol) drop by drop with a syringe at -78 °C. The solution was warmed to ambient temperature and stirred for 1 h, during which time a gradual color change from brown to red was observed. Subsequently, the solution was quenched by the addition of aqueous NaOH solution (1.5 equiv). The resulting yellow solution was filtered, and all volatiles were removed in vacuo. The residue was washed with hexane and then dried in vacuo to give **5d** (240 mg, 86%). This procedure is also applicable to the synthesis of **5a**. Spectral data for **5a,d** are summarized in Table 7. Prismatic crystals of **5d**, suitable for an X-ray structure determination, were grown from benzene/hexane solution at -10 °C. The instability of **5a,d** has prevented microanalysis.

## ■ ASSOCIATED CONTENT

### ■ Supporting Information

Tables, text, figures, and CIF files giving crystal data and experimental parameters for compounds **3a,3b**, **4a2**, and **5d**, NMR (<sup>1</sup>H, <sup>13</sup>C, and <sup>29</sup>Si) and IR data for all compounds, and NMR (<sup>1</sup>H, <sup>13</sup>C, <sup>31</sup>P, and <sup>29</sup>Si) spectra for **3b,c** and **4a1-4c3** (S3). This material is available free of charge via the Internet at <http://pubs.acs.org>. The data for **3a**, **3b**, **4a2**, and **5d** have also been deposited with Cambridge Crystallographic Data center, as CCDC Nos. 833579 (**3a**), 822146 (**3b**), 172503 (**4a2**), and 81833 (**5d**).

## ■ AUTHOR INFORMATION

### ■ Corresponding Author

\*E-mail: [minato@ynu.ac.jp](mailto:minato@ynu.ac.jp). Tel: +81-45-339-3933. Fax: +81-45-339-3933.

### ■ Present Address

<sup>§</sup>The Institute of Scientific and Industrial Research, Osaka University, Mihogaoka, Ibaraki, Osaka 567-0047, Japan.

### ■ Notes

The authors declare no competing financial interest.

## ■ ACKNOWLEDGMENTS

We are grateful to Dr. M. Yamasaki of Rigaku Corp. for X-ray structure analyses.

## ■ REFERENCES

(1) (a) Tilley, T. D. In *The Chemistry of Organic Silicon Compounds*; Patai, S., Rappaport, Z., Eds.; Wiley: New York, 1989; Part 2, Chapter

24. (b) Tilley, T. D. In *The Silicon-Heteroatom Bond*; Patai, S., Rappaport, Z., Eds.; Wiley: New York, 1991; Chapter 10. (c) Corey, J. Y.; Braddock-Wilking, J. *Chem. Rev.* **1999**, *99*, 175.

(2) (a) Zhou, D.-Y.; Minato, M.; Ito, T.; Yamasaki, M. *Chem. Lett.* **1997**, 1017. (b) Zhou, D.-Y.; Zhang, L.-B.; Minato, M.; Ito, T.; Osakada, K. *Chem. Lett.* **1998**, 187. (c) Kubas, G. J. In *Metal Dihydrogen and σ-Bond Complexes*; Kluwer: New York, 2001; pp 339–340. (d) Minato, M.; Zhou, D.-Y.; Zhang, L.-B.; Hirabayashi, R.; Kakeya, M.; Matsumoto, T.; Harakawa, A.; Kikutsuji, G.; Ito, T. *Organometallics* **2005**, *24*, 3434.

(3) (a) Auburn, M. J.; Holmes-Smith, R. D.; Stobart, S. R. *J. Am. Chem. Soc.* **1984**, *106*, 1314. (b) Auburn, M. J.; Grundy, S. L.; Stobart, S. R.; Zaworotko, M. J. *J. Am. Chem. Soc.* **1985**, *107*, 266. (c) Auburn, M. J.; Stobart, S. R. *Inorg. Chem.* **1985**, *24*, 318. (d) Holmes-Smith, R. D.; Stobart, S. R.; Vefghi, R.; Zaworotko, M. J.; Jochem, K.; Cameron, T. S. *J. Chem. Soc., Dalton Trans.* **1987**, 969. (e) Okazaki, M.; Ohshitanai, S.; Tobita, H.; Ogino, H. *Chem. Lett.* **2001**, 952. (f) Okazaki, M.; Tobita, H.; Ogino, H. *J. Chem. Soc., Dalton Trans.* **2002**, 2061. (g) Sangtrirutnugul, P.; Stradiotto, M.; Tilley, T. D. *Organometallics* **2006**, *25*, 1607.

(4) (a) Takaya, J.; Iwasawa, N. *J. Am. Chem. Soc.* **2008**, *130*, 15254. (b) MacInnis, M.; McDonald, R.; Ferguson, M. J.; Tobisch, S.; Turculet, L. *J. Am. Chem. Soc.* **2011**, *133*, 13622. (c) Lee, Y.; Peters, J. *J. Am. Chem. Soc.* **2011**, *133*, 4438.

(5) (a) Chatt, J.; Eaborn, C.; Ibekwe, S. *J. Chem. Soc., Chem. Commun.* **1966**, 700. (b) McWeeny, R.; Mason, R.; Towl, A. D. C. *Discuss. Faraday Soc.* **1969**, *47*, 20. (c) Haszeldine, R. N.; Parish, R. V.; Setchfield, J. H. *J. Organomet. Chem.* **1973**, *57*, 279.

(6) (a) Minato, M.; Nishiuchi, J.; Kakeya, M.; Matsumoto, T.; Yamaguchi, Y.; Ito, T. *Dalton Trans.* **2003**, 483. (b) Minato, M.; Kikutsuji, G.; Kakeya, M.; Osakada, K.; Yamasaki, M. *Dalton Trans.* **2009**, 7684.

(7) Minato, M.; Zhou, D.-Y.; Sumiura, K.; Hirabayashi, R.; Yamaguchi, Y.; Ito, T. *Chem. Commun.* **2001**, 2654.

(8) (a) Dickman, M. H.; Pope, M. T. *Chem. Rev.* **1994**, *94*, 569. (b) Kitajima, N.; Fujisawa, K.; Fujimoto, C.; Moro-oka, Y.; Hashimoto, S.; Kitagawa, T.; Toriumi, T.; Tatsumi, K.; Nakamura, A. *J. Am. Chem. Soc.* **1992**, *114*, 1277.

(9) Mezzetti, A.; Zangrando, E.; Del Zotto, A.; Rigo, P. *Chem. Commun.* **1994**, 1597.

(10) Legzdins, P.; Phillips, E. C.; Rettig, C. J.; Sánchez, L.; Trotter, J.; Yee, V. C. *Organometallics* **1988**, *7*, 1877.

(11) Cotton, F. A.; Wilkinson, G. In *Advanced Inorganic Chemistry*, 5th ed.; Wiley: New York, 1988; p 469.

(12) Nakamoto, K. In *Infrared and Raman Spectra of Inorganic and Coordination Compounds*, 3rd ed.; Wiley: New York, 1977; pp 230–233.

(13) Ito, T.; Takahashi, A.; Tamura, S. *Bull. Chem. Soc. Jpn.* **1986**, *59*, 3489.

(14) Ito, T.; Matsubara, T.; Yamashita, Y. *J. Chem. Soc., Dalton Trans.* **1990**, 2407.

(15) Ito, T.; Shimada, K.; Ono, T.; Minato, M.; Yamaguchi, Y. *J. Organomet. Chem.* **2000**, *611*, 308.

(16) Sneed, R. P. A. In *Comprehensive Organometallic Chemistry*; Wilkinson, G., Ed.; Pergamon Press: Oxford, U.K., 1982; Vol. 8, pp 225–283.

(17) Ito, T.; Matsubara, T. *J. Chem. Soc., Dalton Trans.* **1988**, 2241.

(18) Jessop, P. G.; Ikariya, T.; Noyori, R. *Chem. Rev.* **1995**, *95*, 259 and references cited therein.

(19) Mitchell, J. A.; Reid, E. E. *J. Am. Chem. Soc.* **1931**, *53*, 1879.

(20) Jessop, P. G.; Hsiao, Y.; Ikariya, T.; Noyori, R. *J. Am. Chem. Soc.* **1994**, *116*, 8851.

(21) Hutschka, H.; Dedieu, A.; Eichberger, M.; Fornika, R.; Leitner, W. *J. Am. Chem. Soc.* **1997**, *119*, 4432.

(22) Beck, W. *Inorg. Synth.* **1990**, *28*, 1 and references cited therein.

(23) Molander, G. A.; Corrette, C. P. *Organometallics* **1998**, *17*, 5504.

(24) Cotton, F. A.; Wilkinson, G. In *Advanced Inorganic Chemistry*, 5th ed.; Wiley: New York, 1988; p 464.

(25) Mine, S.; Minato, M. To be submitted for publication.